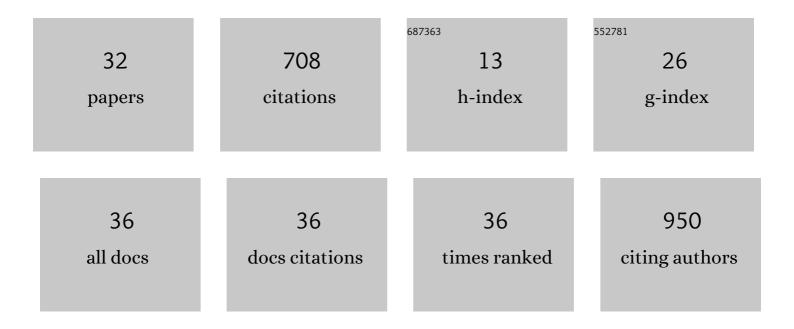
## Rong Wu

## List of Publications by Year in descending order

Source: https://exaly.com/author-pdf/8870013/publications.pdf Version: 2024-02-01



RONG WU

#	Article	IF	CITATIONS
1	Ultrasoundâ€Augmented Nanocatalytic Ferroptosis Reverses Chemotherapeutic Resistance and Induces Synergistic Tumor Nanotherapy. Advanced Functional Materials, 2022, 32, 2107529.	14.9	43
2	The association between conventional ultrasound and contrast-enhanced ultrasound appearances and pathological features in small breast cancer. Clinical Hemorheology and Microcirculation, 2022, 80, 413-422.	1.7	4
3	Comparison of lymphatic contrast-enhanced ultrasound and intravenous contrast-enhanced ultrasound in the preoperative diagnosis of axillary sentinel lymph node metastasis in patients with breast cancer. British Journal of Radiology, 2022, 95, 20210897.	2.2	4
4	Diagnostic value of Doppler imaging for malignant non-mass breast lesions: with different diagnostic criteria for older and younger women: first results. Clinical Hemorheology and Microcirculation, 2022, 81, 123-134.	1.7	1
5	Enhancing Non-Mass Breast Ultrasound Cancer Classification with Knowledge Transfer. , 2022, , .		0
6	Self Supervised Lesion Recognition for Breast Ultrasound Diagnosis. , 2022, , .		1
7	Ultrasonic multimodality imaging features and the classification value of nonpuerperal mastitis. Journal of Clinical Ultrasound, 2022, , .	0.8	2
8	Ultrasound-enhanced fluorescence imaging and chemotherapy of multidrug-resistant tumors using multifunctional dendrimer/carbon dot nanohybrids. Bioactive Materials, 2021, 6, 729-739.	15.6	58
9	Engineering two-dimensional silicene composite nanosheets for dual-sensitized and photonic hyperthermia-augmented cancer radiotherapy. Biomaterials, 2021, 269, 120455.	11.4	36
10	Conventional and contrast-enhanced ultrasound features in sclerosing adenosis and correlation with pathology. Clinical Hemorheology and Microcirculation, 2021, 77, 173-181.	1.7	6
11	Two-dimensional LDH nanodisks modified with hyaluronidase enable enhanced tumor penetration and augmented chemotherapy. Science China Chemistry, 2021, 64, 817-826.	8.2	16
12	Tumor-derived exosomal long noncoding RNA LINC01133, regulated by Periostin, contributes to pancreatic ductal adenocarcinoma epithelial-mesenchymal transition through the Wnt/β-catenin pathway by silencing AXIN2. Oncogene, 2021, 40, 3164-3179.	5.9	45
13	Application of ultrasonic dual-mode artificially intelligent architecture in assisting radiologists with different diagnostic levels on breast masses classification. Diagnostic and Interventional Radiology, 2021, 27, 315-322.	1.5	11
14	Predictive value of contrast-enhanced ultrasound combined with conventional ultrasound in solid renal parenchymal lesions. British Journal of Radiology, 2021, 94, 20210518.	2.2	2
15	Incorporation of contrast-enhanced ultrasound in the differential diagnosis for breast lesions with inconsistent results on mammography and conventional ultrasound. Clinical Hemorheology and Microcirculation, 2020, 74, 463-473.	1.7	13
16	Quantitative Measurement of Metal Accumulation in Brain of Patients With Wilson's Disease. Movement Disorders, 2020, 35, 1787-1795.	3.9	15
17	ERas regulates cell proliferation and epithelial–mesenchymal transition by affecting Erk/Akt signaling pathway in pancreatic cancer. Human Cell, 2020, 33, 1186-1196.	2.7	3
18	Engineering of SPECT/Photoacoustic Imaging/Antioxidative Stress Triple-Function Nanoprobe for Advanced Mesenchymal Stem Cell Therapy of Cerebral Ischemia. ACS Applied Materials & Interfaces, 2020, 12, 37885-37895.	8.0	36

Rong Wu

#	Article	IF	CITATIONS
19	Diagnostic efficacy of contrast-enhanced ultrasound for breast lesions of different sizes: a comparative study with magnetic resonance imaging. British Journal of Radiology, 2020, 93, 20190932.	2.2	8
20	Ultrasound-targeted microbubble destruction optimized HGF-overexpressing bone marrow stem cells to repair fibrotic liver in rats. Stem Cell Research and Therapy, 2020, 11, 145.	5.5	17
21	The Long-Term Fate of the Sonoporated Pancreatic Cancer Cells is Uncorrelated With the Degree of Model Molecular Loading. Ultrasound in Medicine and Biology, 2020, 46, 1015-1025.	1.5	2
22	Qualitative analysis of contrast-enhanced ultrasound in the diagnosis of small, TR3–5 benign and malignant thyroid nodules measuring â‰ቑ cm. British Journal of Radiology, 2020, 93, 20190923.	2.2	17
23	Quantifying Levator Ani Muscle Elasticity Under Normal and Prolapse Conditions by Shear Wave Elastography. Journal of Ultrasound in Medicine, 2020, 39, 1379-1388.	1.7	19
24	Diagnostic Performance of Ultrasound Shear Wave Elastography in Solid Small (â‰ <b>¤</b> cm) Renal Parenchymal Masses. Ultrasound in Medicine and Biology, 2019, 45, 2328-2337.	1.5	9
25	Relation between carotid vulnerable plaques and peripheral leukocyte: a case-control study of comparison utilizing multi-parametric contrast-enhanced ultrasound. BMC Medical Imaging, 2019, 19, 74.	2.7	6
26	Ultrasmall Cu2-xS nanodots as photothermal-enhanced Fenton nanocatalysts for synergistic tumor therapy at NIR-II biowindow. Biomaterials, 2019, 206, 101-114.	11.4	223
27	Radiofrequency-Sensitive Longitudinal Relaxation Tuning Strategy Enabling the Visualization of Radiofrequency Ablation Intensified by Magnetic Composite. ACS Applied Materials & Interfaces, 2019, 11, 11251-11261.	8.0	42
28	Ultrasound findings of urachal anomalies. A series of interesting cases. Medical Ultrasonography, 2019, 21, 294.	0.8	10
29	Mesoporeâ€Induced Aggregation of Cobalt Protoporphyrin for Photoacoustic Imaging and Antioxidant Protection of Stem Cells. Advanced Functional Materials, 2018, 28, 1804497.	14.9	21
30	Reduction of HIP2 expression causes motor function impairment and increased vulnerability to dopaminergic degeneration in Parkinson's disease models. Cell Death and Disease, 2018, 9, 1020.	6.3	17
31	Traditional Chinese medicine for modern treatment of Parkinson's disease. Chinese Journal of Integrative Medicine, 2017, 23, 635-640.	1.6	15
32	A comparison study of local injection and radiofrequency ablation therapy for traumatic portal vein injure guided by contrast-enhanced ultrasonography. Annals of Hepatology, 2012, 11, 249-256.	1.5	6